

FIG. 2. Data for cylinder 2 taken at 10 000 cps with 3 sec integration time and 14 min field sweep. The average slope of the curve is attributed to the Meissner effect of the walls of this cylinder which were approximately ten times thicker than those of cylinder 1.

Since the voltage across the pickup coil is proportional to the flux change occurring as the cylinder becomes superconducting in the presence of the magnetic field, it can be interpreted as a measure of the equilibrium magnetization of the cylinder in the presence of the field. These magnetization data correspond to the point-by-point magnetization measurements of the original experiments of Deaver and Fairbank¹ in which both the magnetization and the trapped flux were found to be periodic functions of the applied field with period $hc/2e$.

When the cylinder is cooled through its superconducting transition temperature in the presence of a magnetic field, a current is induced in the walls to achieve the nearest integral number of quanta within the cylinder. Thus, when the cylinder is cooled in an applied field producing less than one-half flux unit within it, the cylin-

der acts as a perfect diamagnet expelling all the flux within it. For a value of applied field producing approximately one-half flux unit within the cylinder a sudden transition is made to the state in which one full flux unit is trapped. When the cylinder is cooled in values of field larger than that necessary to produce one unit, the excess flux over one unit is expelled.

It continues to trap one unit until an applied field producing approximately one and one-half flux units within the cylinder is reached, at which field a sudden transition to two quanta trapped is made. This pattern repeats as a function of field, and for a very thin-walled cylinder produces a sawtooth-shaped magnetization curve. For a thick-walled cylinder the curve has an average slope corresponding to the Meissner effect of the walls, which is proportional to $H_{\text{applied}} \times (\text{wall area})$.

The exact shape of the magnetization curves obtained in these measurements is probably influenced by nonuniformities in the size of the cylinder and in variations of thermal response along the length of the cylinder.

The authors wish to express their gratitude to Professor W. M. Fairbank for many stimulating and enlightening discussions.

*Work supported in part by the U. S. Office of Naval Research and in part by the Air Force Office of Scientific Research.

†Present address: Chemistry Department, Harvard University, Cambridge, Massachusetts.

¹B. S. Deaver, Jr., and W. M. Fairbank, *Phys. Rev. Letters* **7**, 43 (1961).

²R. Doll and M. Näbauer, *Phys. Rev. Letters* **7**, 51 (1961).

³J. E. Mercereau and L. L. Vant-Hull, *Bull. Am. Phys. Soc.* **6**, 121 (1961).

SPIN-DENSITY-WAVE ANTIFERROMAGNETISM IN POTASSIUM

A. W. Overhauser

Scientific Laboratory, Ford Motor Company, Dearborn, Michigan
(Received 8 July 1964)

It is shown that the recently discussed¹ optical-absorption threshold in metallic K, found by El Naby² at $\hbar\omega = 0.62$ eV, provides striking evidence that the electronic state of the metal is a giant spin-density-wave state. The optical absorption associated with the spin-density-wave energy gap is calculated and found to be in remarkable quantitative agreement with the observed spectrum. Direct observation of the spin-density

wave by neutron diffraction is feasible, since its amplitude is estimated to be 0.09 Bohr magneton per atom.

In the Hartree-Fock (HF) approximation the normal state of every metal is unstable with respect to spin-density-wave (SDW) formation.³ However, without an exact solution of the many-body problem, the presence of an SDW can be surmised only from experimental evidence,

direct (as in³ Cr) or indirect (as in Cu, Ag, and⁴ Au). Low electron density favors their formation, so the alkali metals may be expected to exhibit them in a more pronounced way compared to most other metals.

Within the HF scheme SDW energy gaps should truncate the Fermi surface, thereby altering the Fermi surface topology by neck formation.³ However, correlation energy considerations lead to the conclusion that for a simple metal an SDW energy gap should touch the Fermi surface only at a single point, as shown in Fig. 1. The argument is as follows: The correlation energy arises from virtual electronic excitations near the Fermi surface. As long as E vs K is continuous at the Fermi surface, low-energy virtual excitations, arising from electron interactions, can occur easily and contribute to the binding energy. If the wave vector \vec{Q} of the SDW is small enough so that a finite area of Fermi surface is truncated by the energy gap, the virtual excitations will be locally inhibited and the correlation energy reduced in magnitude. The net effect is a repulsion between the Fermi surface and the energy gaps, which allows the total energy to be a minimum when the gaps just touch the Fermi surface. (One needs to remember that the HF energy leads to a small attractive interaction between the Fermi surface and the energy gaps.³)

We will now compute the optical absorption associated with a single linear SDW. The periodic exchange potential causing the energy gaps is

$$A(\vec{r}) = G\vec{u} \cdot \vec{\sigma} \cos \vec{Q} \cdot \vec{r}, \quad (1)$$

where $\vec{\sigma}$ is the Pauli spin operator and \vec{u} is the SDW polarization vector. The one-electron energy E_K obtained by including (1) in the Schrödinger equation is the familiar result of weak-binding theory. In the vicinity of the gap at A (Fig. 1),

$$E_K = \epsilon_K + \mu z \pm (\mu^2 z^2 + G^2/4)^{1/2}, \quad (2)$$

where z is the perpendicular distance in K space from the gap, $\epsilon_K = \hbar^2 K^2/2m$, and $\mu = \hbar^2 Q/2m$. The space parts of the wave functions above and below the gap, respectively (for spin parallel to \vec{u}), are

$$\varphi_K = \cos \theta \exp i \vec{K} \cdot \vec{r} + \sin \theta \exp i (\vec{K} + \vec{Q}) \cdot \vec{r}, \quad (3a)$$

$$\varphi_{K'} = \sin \theta \exp i \vec{K}' \cdot \vec{r} - \cos \theta \exp i (\vec{K}' + \vec{Q}) \cdot \vec{r}, \quad (3b)$$

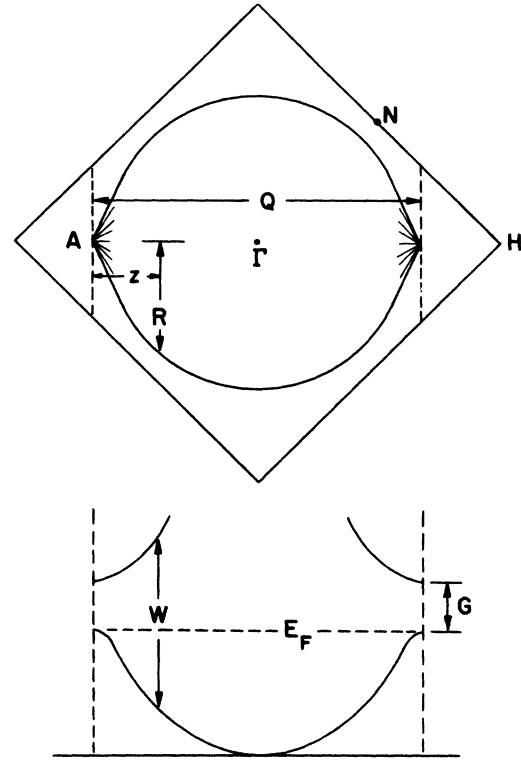


FIG. 1. Brillouin zone, Fermi surface, and electron energy spectrum of potassium with a single linear spin-density-wave state. The wave vector of the spin-density wave is assumed to be parallel to a cubic axis.

where

$$\sin \theta \cos \theta = G/2W, \quad (4)$$

and

$$W = 2(\mu^2 z^2 + G^2/4)^{1/2} \quad (5)$$

is the vertical transition energy. The radius R of the Fermi surface at z is found with the help of (2), (5), and the condition $R=0$ at $z=0$:

$$\frac{R^2}{Q^2} = \frac{W-G}{2\mu Q} \left(1 - \frac{W+G}{2\mu Q} \right). \quad (6)$$

Consider now a light wave traveling in the ζ direction of a centimeter cube of metal. The vector potential may be taken to be

$$\vec{A} = \vec{v} \exp[(in - k)(\omega \zeta/c) - i\omega t], \quad (7)$$

where n and k are the optical constants, and \vec{v} is the polarization vector. The energy flux at the front surface, $\zeta=0$, is accordingly

$$P = (c/4\pi) \text{Re}(\vec{E}^* \times \vec{H}) = n\omega^2/4\pi c. \quad (8)$$

We need only compute the SDW band-to-band transition rate caused by the perturbation, V

$= (e/mc)\vec{A}\cdot\vec{p}$, and set the result equal to P divided by $W = \hbar\omega$:

$$\frac{P}{W} = 4 \sum_{K', K} (2\pi/\hbar) |V_{K'K}|^2 \delta(E_K - E_{K'} - \hbar\omega), \quad (9)$$

where the factor 4 takes account of the spin degeneracy and the two gaps at opposite sides of the Fermi surface. Employing (3), one finds

$$|V_{KK'}|^2 = (e\hbar\vec{v}\cdot\vec{Q}\sin\theta\cos\theta/mc)^2 \times [(K_{\zeta}' - K_{\zeta} + \omega n/c)^2 + (\omega k/c)^2]^{-1}, \quad (10)$$

the \vec{K} components transverse to ζ being conserved. The double sum in (9) can be evaluated:

$$\frac{P}{W} = \frac{c}{2\pi^2 W k} \left(\frac{e\hbar Q G \cos\alpha}{2mcW} \right)^2 \pi R^2 \frac{dz}{dW}, \quad (11)$$

where α is the angle between \vec{v} and \vec{Q} . With the help of (5), (6), and (8), the imaginary part, $2nk$, of the dielectric constant is found:

$$2nk = \frac{G^2 e^2 Q}{3W^3} \left(\frac{W-G}{W+G} \right)^{1/2} \left(1 - \frac{W+G}{2\mu Q} \right), \quad (12)$$

where $\cos^2\alpha$ has been replaced by its average value, $\frac{1}{3}$.

It is emphasized that the final result (12) has no adjustable parameter other than the threshold energy G . Equation (6) can be used to find Q , which is slightly larger than the diameter, $2k_F$

$= 1.24(2\pi/a)$, of the undeformed Fermi sphere:

$$Q = 1.33(2\pi/a), \quad (13)$$

where a is the lattice constant. The theoretical absorption coefficient, $2nk/\lambda$, is shown in Fig. 2 for $G = 0.62$ eV. The experimental data of El Naby,² after subtracting the Drude background,⁵ are also shown. The remarkable agreement, both as to shape and absolute magnitude, indicates that potassium has a single linear SDW. The peculiar absorption shape is characteristic of interband transitions at an energy gap which touches the Fermi surface at a single point. (A truncated face of finite area yields a singular absorption behavior above threshold, whereas a gap which does not touch at all causes a linear rise above threshold.) The absorption anomaly cannot be ascribed to the Fermi surface touching the 12 zone faces (at N) since that would require a sixfold larger magnitude.

Possible difficulties in observing SDW's by neutron diffraction have been discussed.³ However, it is anticipated that direct observation in this case should be easy. The fractional spin polarization of the SDW can be computed using the observed G . The amplitude is found to be 9%, which is adequately large provided the SDW has transverse polarization. This should be the case for a simple metal like K, since the magnetostatic energy favors transverse polarization, and the situation is not complicated by multiple SDW interactions. The direction of \vec{Q} is probably either the cubic axis or the body diagonal. Consequently, a single SDW domain should exhibit a slight tetragonal (or rhombohedral) distortion. However, the optical properties of a domain should be highly anisotropic, since the anomalous absorption is proportional to $\cos^2\alpha$.

Near a point of contact with the energy gaps, the Fermi surface has the shape of a circular cone with semivertical angle β given by

$$\tan\beta = [(\mu Q/G) - 1]^{1/2}. \quad (14)$$

For potassium, $\beta = 75^\circ$. Several anomalies⁶ in the cyclotron resonance of K may possibly arise from the conical shape of the Fermi surface at such points.

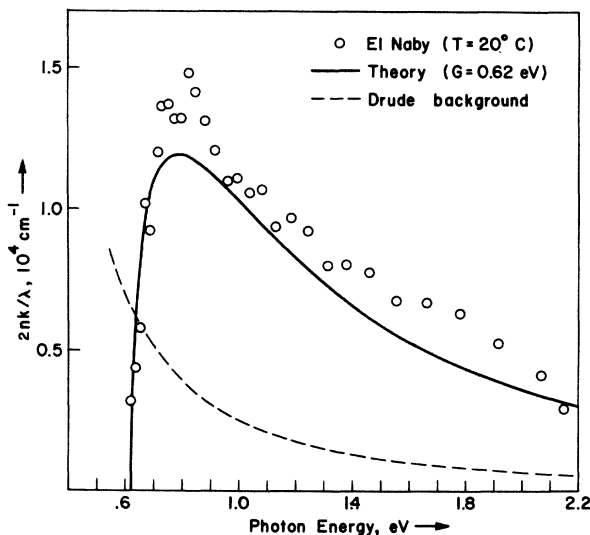


FIG. 2. Optical-absorption spectrum of potassium. The theoretical curve, according to Eq. (12) of the text, has no adjustable parameter other than the threshold energy G . The experimental values shown are those obtained after subtracting the Drude background.

¹M. H. Cohen and J. C. Phillips, Phys. Rev. Letters **12**, 662 (1964).

²M. H. El Naby, Z. Physik **174**, 269 (1963).

³A. W. Overhauser, Phys. Rev. **128**, 1437 (1962).

⁴L. L. Van Zandt and A. W. Overhauser, Bull. Am. Phys. Soc. **8**, 337 (1963), and to be published; L. L. Van Zandt, thesis, Harvard University, 1964 (unpublished).

⁵H. Mayer and M. H. El Naby, Z. Physik **174**, 289 (1963).

⁶C. C. Grimes and A. F. Kip, Phys. Rev. **132**, 1991 (1963).

ELECTROABSORPTION SPECTRUM IN SILICON

Marvin Chester and Paul H. Wendland
University of California, Los Angeles, California
(Received 18 June 1964)

In examining the absorption spectral response of silicon in the presence of an electric field we have seen some hitherto unreported structure. Our differential technique yields measurements of the change $\Delta\alpha$ in the absorption coefficient α , arising from the application of an electric field F to the specimen. Figure 1 shows curves of $\Delta\alpha$ vs photon energy for two different values of applied field. We have been exploring the 0.9- to 1.5-micron region of the spectrum where the absorption edge due to electron interband transitions begins. The experiments were performed at room temperature.

The specimens, made of 400- to 600-ohm-cm *p*-type silicon, were single-crystal-hyperpure 10-mil wafers lapped in the (111) plane, obtained from Dow Corning Corporation. These wafers were optically polished on both sides to a thickness of 4-5 mils and etched in CP-4 to a final thickness of 1-3 mils. After a thorough wash in de-ionized water, they were dried and an epoxy edge protection was applied. A transparent gold

layer was evaporated on one side and a transparent aluminum layer on the opposite side of the wafer. The field was applied between these two transparent electrodes. This sample preparation technique, except for the transparent aluminum electrode, follows closely that described^{1,2} for constructing surface-barrier nuclear particle detectors. We have used this construction in order to produce high electric fields in the samples without driving high currents through them. This is achieved by applying the field in the reverse bias direction. Using samples at room temperature without a surface barrier or with forward-bias fields, the shift of the absorption edge due to large current ohmic heating masks the high-field effects. With 50 to 100 volts across these samples, they are fully depleted. Thus we operate in a range where the field strength through the specimen is given by the applied voltage divided by the sample thickness.

A differential technique was used to measure the small change in absorption which occurs upon application of an electric field (see Fig. 2). Steady unchopped light from a Bausch and Lomb high-intensity grating monochromator was focused on the Si sample located a few millimeters away from the exit slit. Square-wave voltage pulses were applied to the sample with a frequency of 50 cps and a duty cycle of 10%. The field variations produced by these pulses changed the ab-

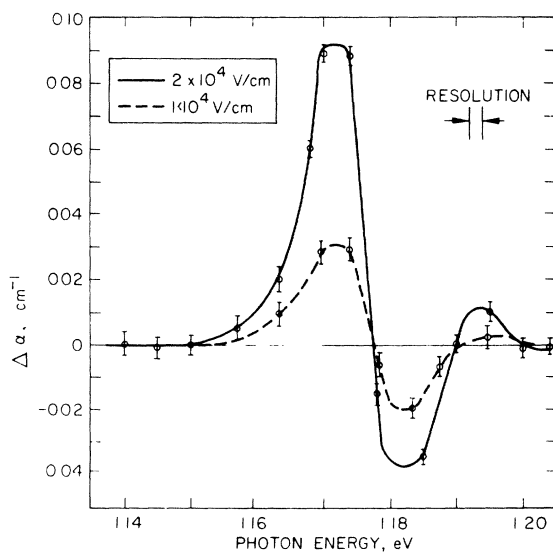


FIG. 1. Electric-field-induced absorption difference vs photon energy.

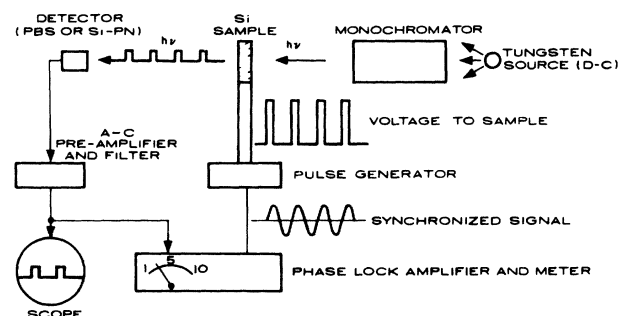


FIG. 2. Differential measurement system.